

**SEISMIC HAZARD STUDIES FOR THE  
ELECTRIC POWER RESEARCH INSTITUTE -  
HIGH LEVEL WASTE PROJECT**

**Kevin J. Coppersmith**

**Geomatrix Consultants  
San Francisco, CA**

**U.S. Nuclear Waste Technical Review Board  
Panel on Structural Geology and Geoengineering**

**Irvine, CA**

**January 22-23, 1992**

## **EPRI-HLW PROJECT OBJECTIVES**

- **To develop an integrated methodology for early site performance assessment and to identify and prioritize crucial issues**
- **To involve DOE in this methodology development and its implementation**

## **EPRI-HLW PROJECT MILESTONES**

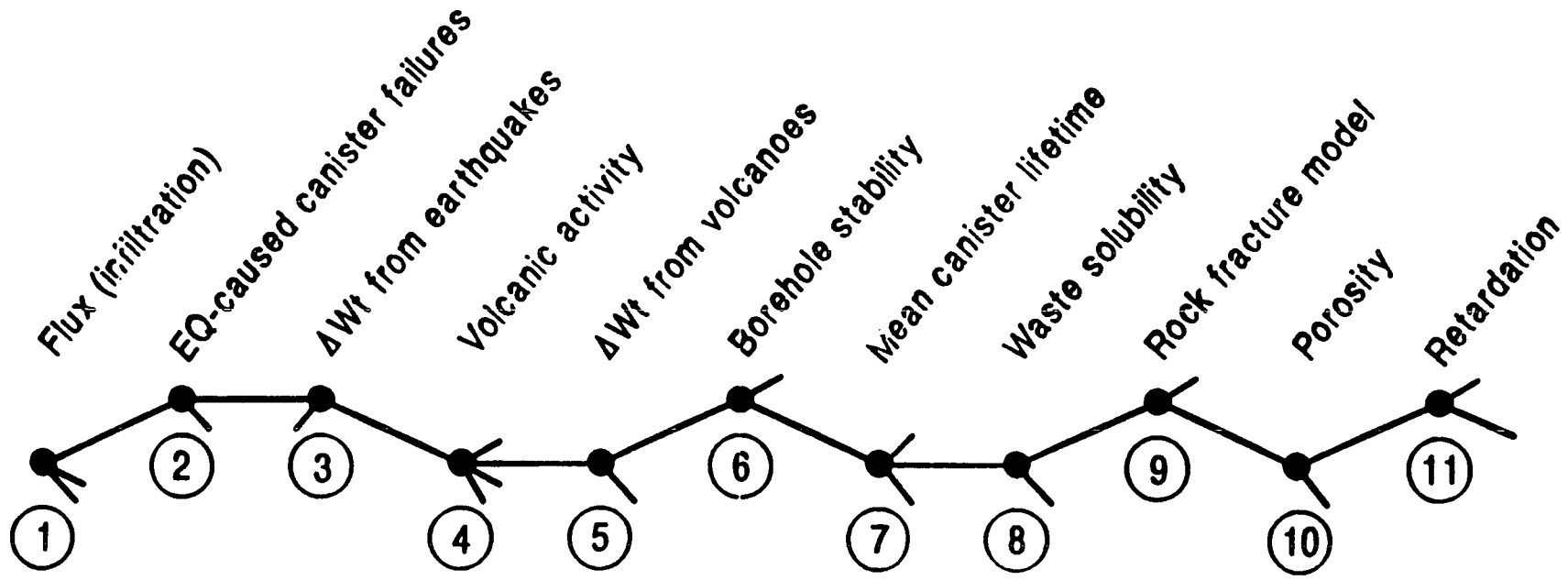
- **Phase 1: Development of methodology for integrated performance assessment (EPRI publication, 1990)**
- **Phase 2: Refinement of methodology including additional elements (EPRI publication, February, 1992)**
- **Phase 3: Demonstration of methods for quantifying uncertainty using earthquakes and tectonics node of master logic tree (EPRI publication, September, 1992)**

## EPRI High Level Waste Project Methodology Development Team

<u>Name</u>	<u>Affiliation</u>	<u>Expertise</u>
Michael J. Apted	Intera Sciences	
Daniel B. Bullen	Georgia Tech	Waste Package
Stuart Childs	Cascade Earth Sciences, Ltd.	Infiltration
Neville Cook	Univ. of Calif, Berkeley	Rock Mechanics
Kevin Coppersmith	Geomatrix Consultants	Seismic Geology
Ralph L. Keeney	Univ. of Southern California	Risk/Decision Analysis
John M. Kemeny	University of Arizona	Rock Mechanics
Austin Long	University of Arizona	Climatology
Robin K. McGuire	Risk Engineering	Risk Analysis
F. Joseph Pearson, Jr.	Consultant	Geochemistry
Benjamin Ross	Disposal Safety, Inc.	Gaseous Transport
Frank W. Schwartz	Ohio State University	Hydrology
Michael Sheridan	State Univ. of NY, Buffalo	Volcanology
Robert A. Shaw	EPRI	Project Manager
J. Carl Stepp	EPRI	Seismology & Geophysics
Robert F. Williams	EPRI	HLW Sciences
Robert Youngs	Geomatrix Consultants	Geotechnical Engineering
Delbert S. Barth	UNLV/ERC	Observer
Russ Dyer	Department of Energy	Observer

**HLW & SFS**

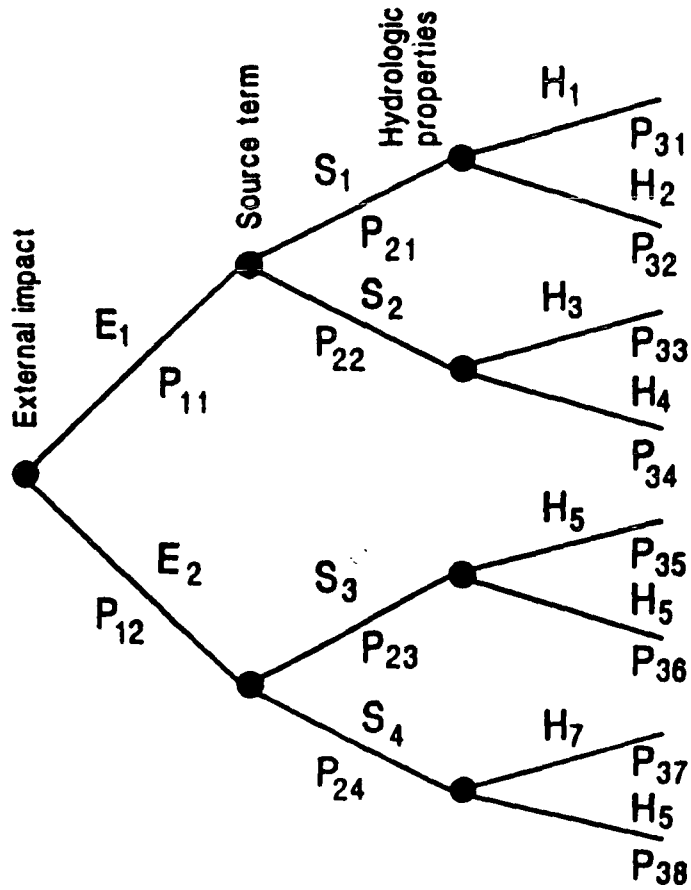
# MASTER LOGIC TREE FOR DEMONSTRATION CALCULATIONS



EQ = Earthquake

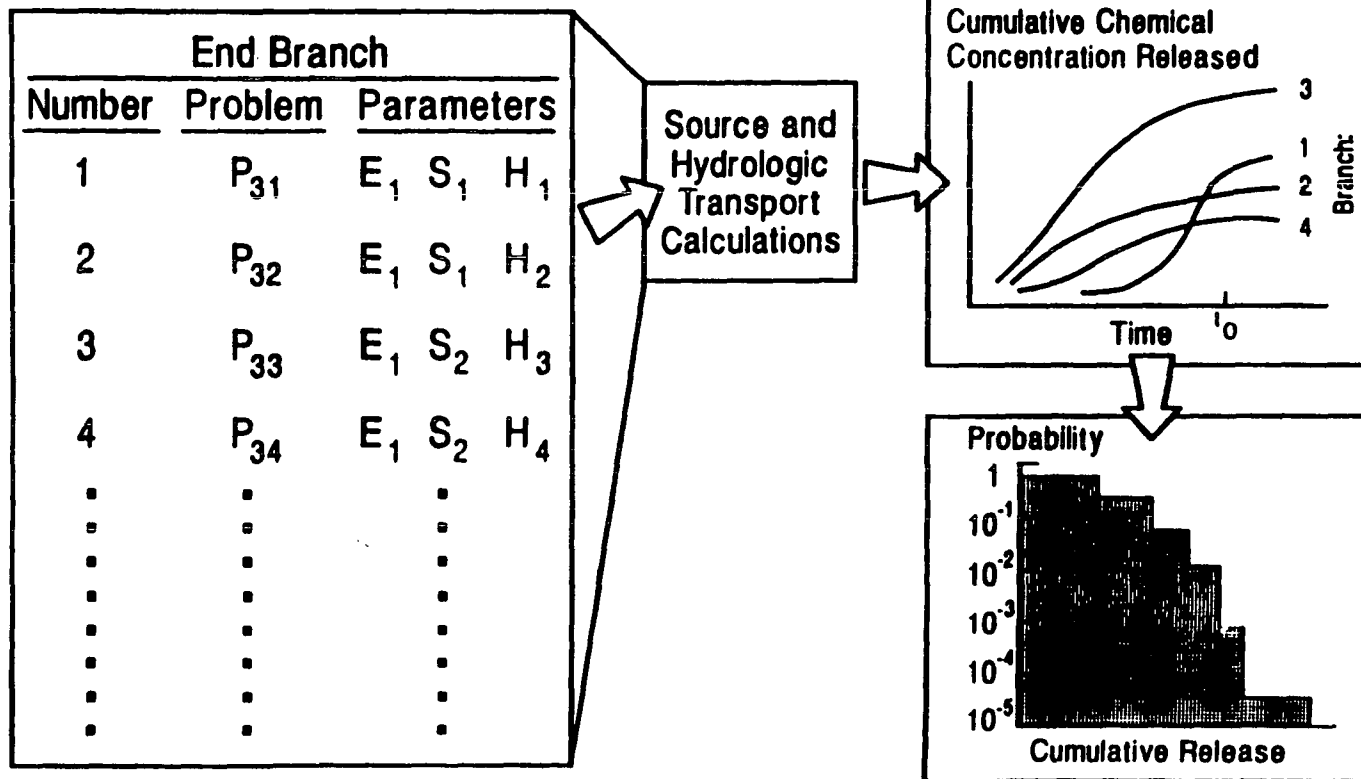
$\Delta Wt$  = Change in water table

# EXAMPLE LOGIC TREE



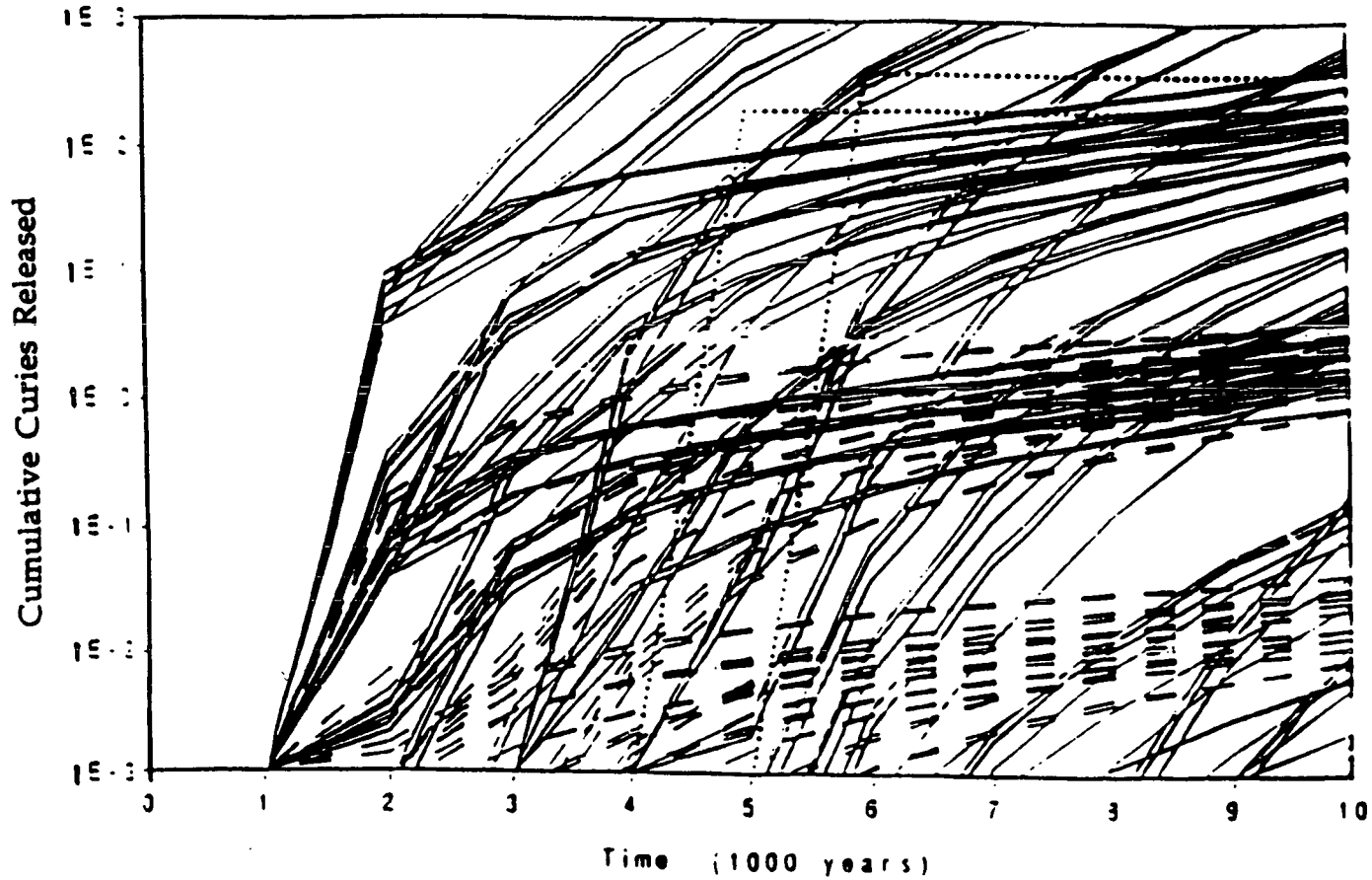
			End Branch		
Number	Problem	Parameters			
1	$P_{31} = P_{11} \times P_{21} \times P_{31}$	$E_1$	$S_1$	$H_1$	
2	$P_{32} = P_{11} \times P_{21} \times P_{32}$	$E_1$	$S_1$	$H_2$	
⋮	⋮	$E_1$	$S_2$	$H_3$	
⋮	⋮	$E_1$	$S_2$	$H_4$	
⋮	⋮	$E_2$	$S_3$	$H_5$	
		$E_2$	$S_3$	$H_6$	
		$E_2$	$S_4$	$H_7$	
		$E_2$	$S_1$	$H_8$	
$\Sigma = 1$					

## LOGIC TREE PARAMETERS TO FORM CCDF OF CUMULATIVE CHEMICAL CONCENTRATION RELEASED



0740.03

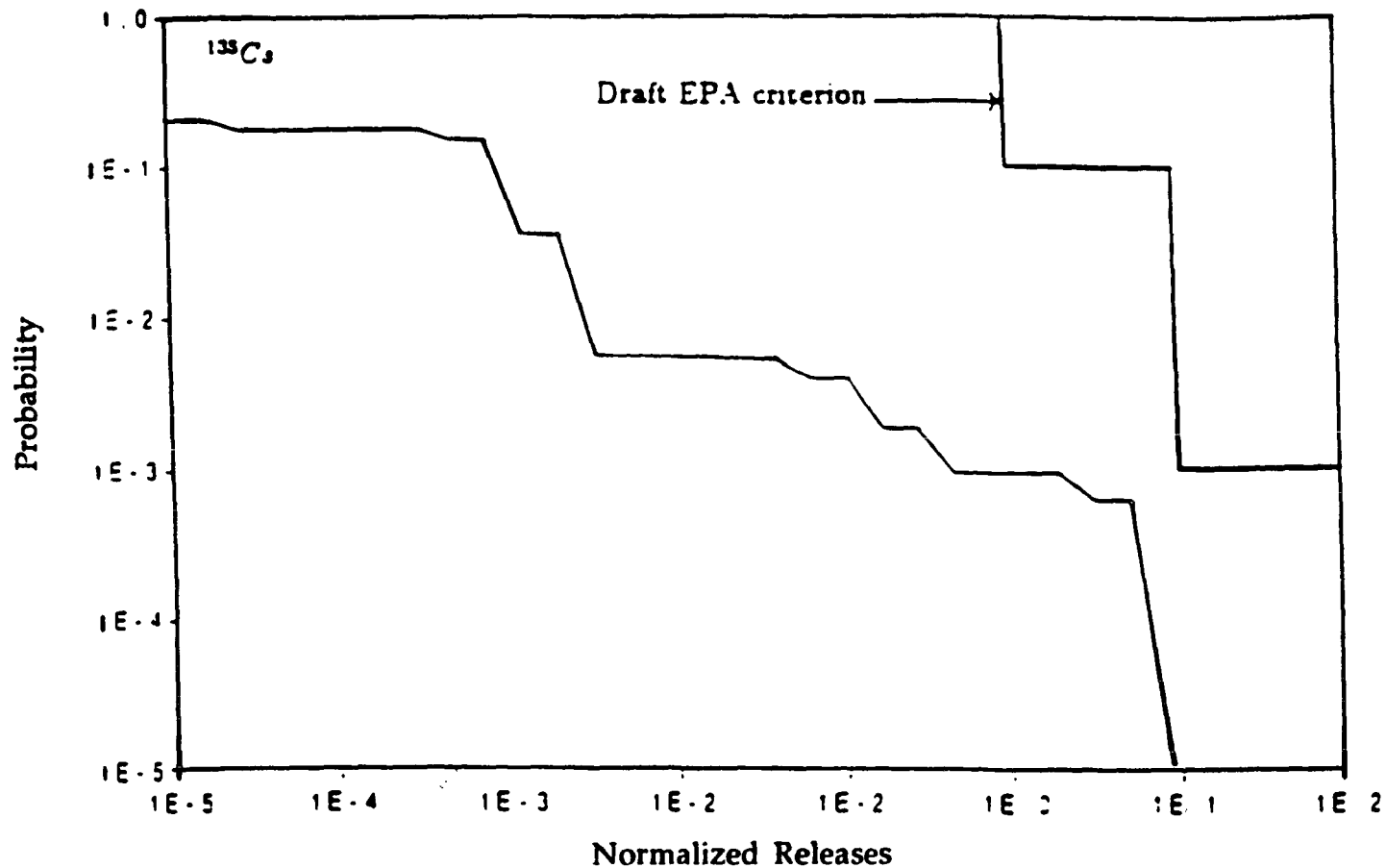
\_\_\_\_\_ FLUX = 4.0 mm/yr  
 \_\_\_\_\_ FLUX = 1.6 mm/yr  
 - - - - - FLUX = 0.5 mm/yr  
 ..... VOLCANIC RELEASE  
<sup>135</sup>Cs      1022 BRANCH FULL CASE



**Cumulative Curies Released vs. Time  
 Showing Sensitivity to Flux**



COMPLEMENTARY CUMULATIVE DISTRIBUTION FUNCTION



**CCDF of Cumulative Curies Released at 10,000 Years  
(Log Probability Axis)**

# **FRAMEWORK FOR ASSESSING FAULT DISPLACEMENT HAZARD**

## **EPRI-HLW PROJECT**

### **Earthquake Source Model**

- **Source identification**
- **Fault activity**
- **Geometry of faults 3-d**
- **Maximum magnitudes for each source**
- **Earthquake recurrence rates for various magnitudes**

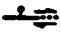
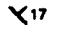
### **Fault Rupture Model**

- **Geometry of primary fault ruptures vv. repository**
- **Distribution of secondary fault ruptures for given primary rupture vv. repository**
- **Probability of intersection with repository**
- **Probability of various amounts of displacement**



Geology compiled from Scott and Bank (1964), Maldonado (1985) and Soodley and Parrish (1988); conceptual repository boundary from Holmes and Narver (1988)

EXPLANATION

- Qac (Quaternary) Alluvium and Colluvium
- Tv (Tertiary) Silicic Volcanic Rocks
-  Fault - dotted where concealed; ball and bar on downthrown side; arrows indicate relative movement
-   $\swarrow 17$  Strike and dip of bedding or foliation

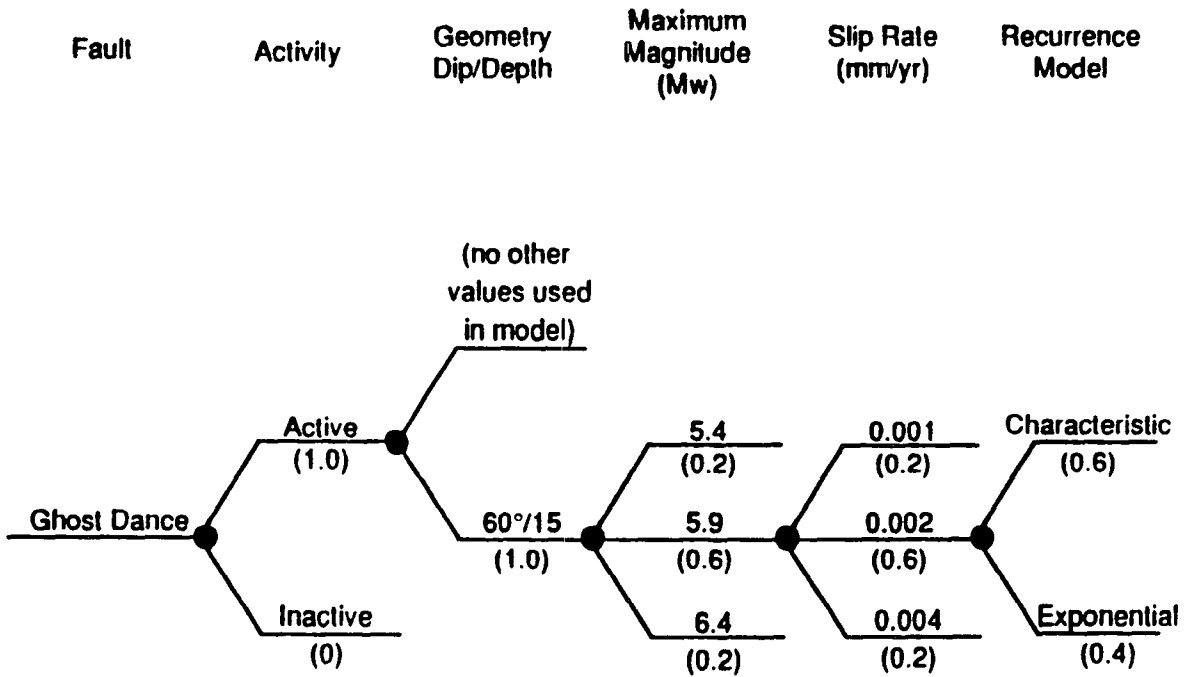




Geology compiled from Scott and Bush (1984), Maldonado (1985), and Swadley and Parrish (1988); conceptual repository boundary from Holmes and Narver (1988).



Generalized geologic map of Midway Valley area.



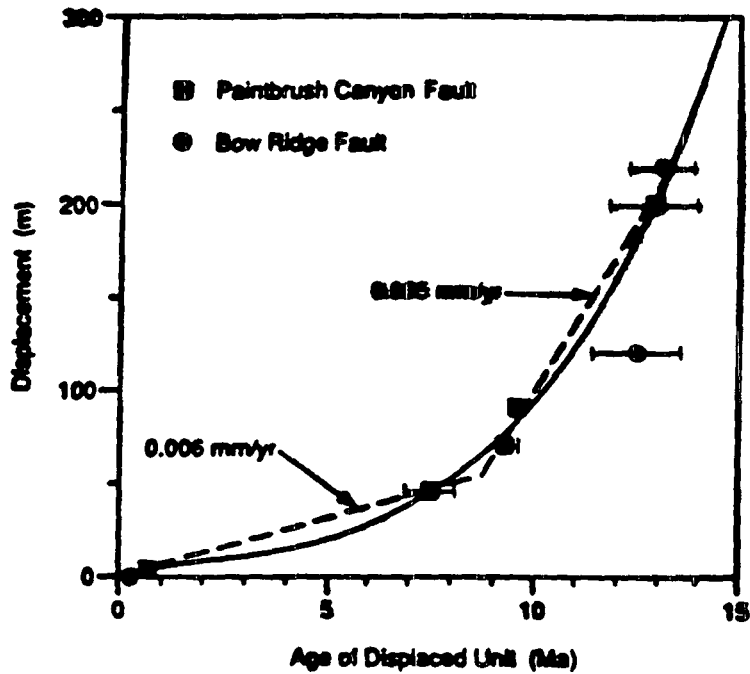
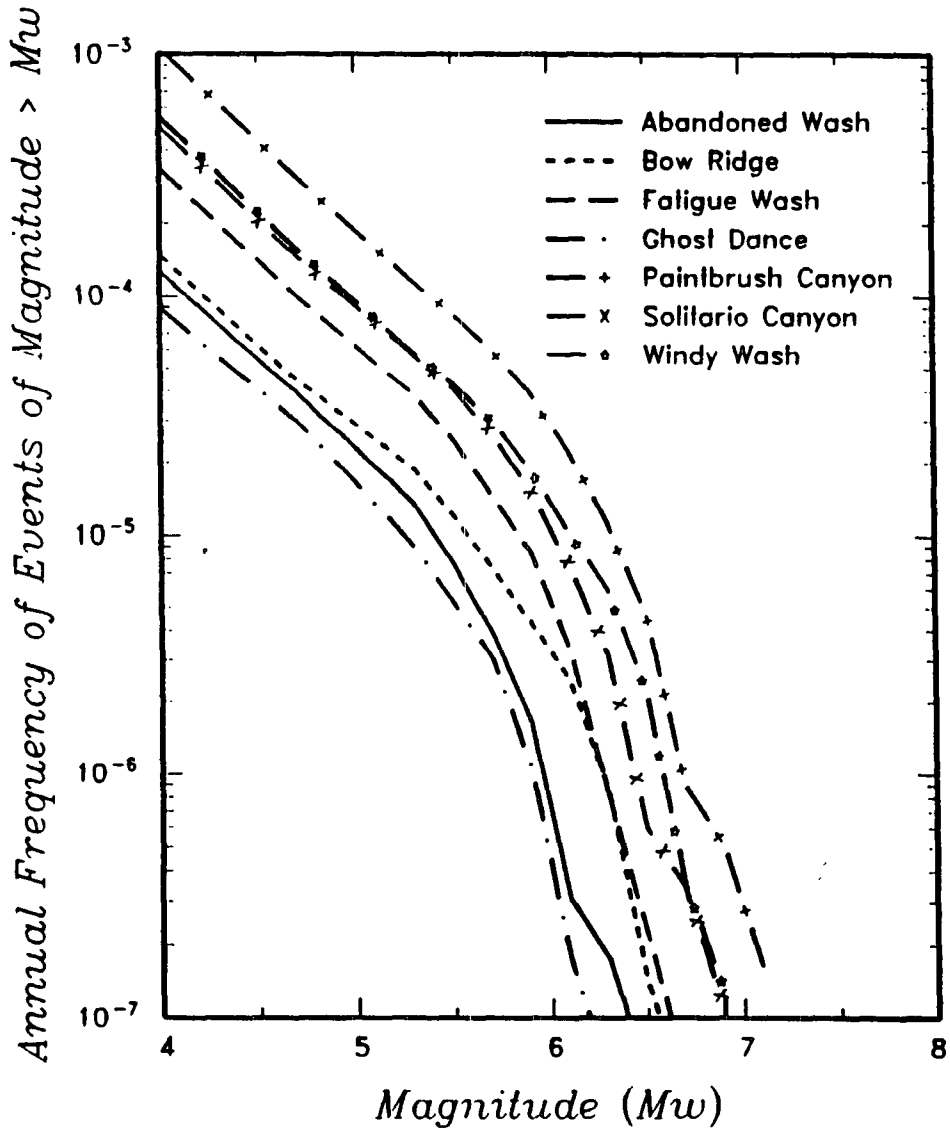
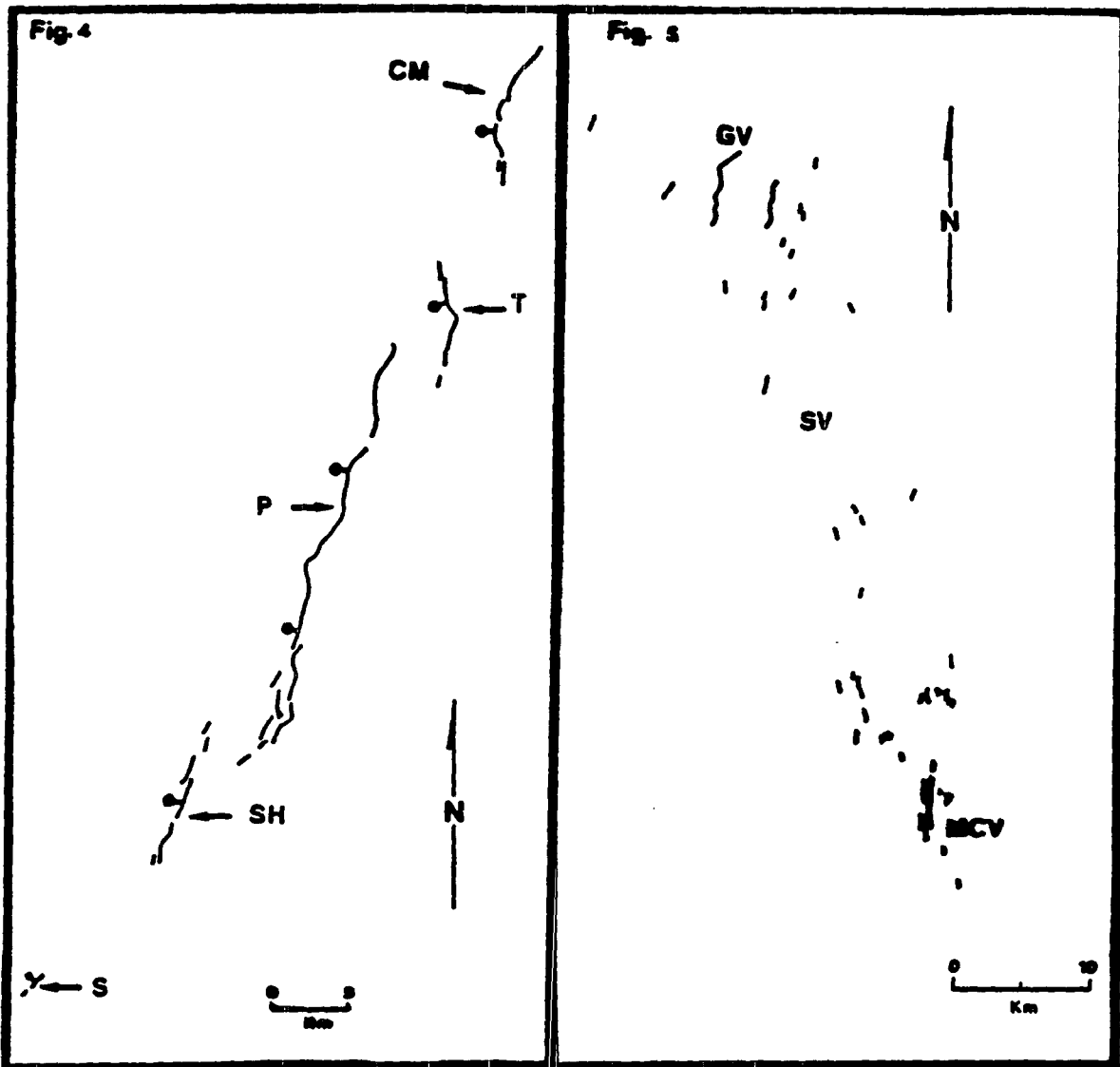


Figure 4. Graph Showing Displacement Versus Age of Displaced Units for the Paintbrush Canyon and Bow Ridge Faults. (Lines are drawn using only the data from the Paintbrush Canyon Fault. The solid line represents a gradual decrease in the rate of slip for the last 10-15 Ma. The dashed lines represent an abrupt change in the slip rate at approximately 8-9 Ma. See Table 1 for data and references.)

*Gibson et al., 1990*



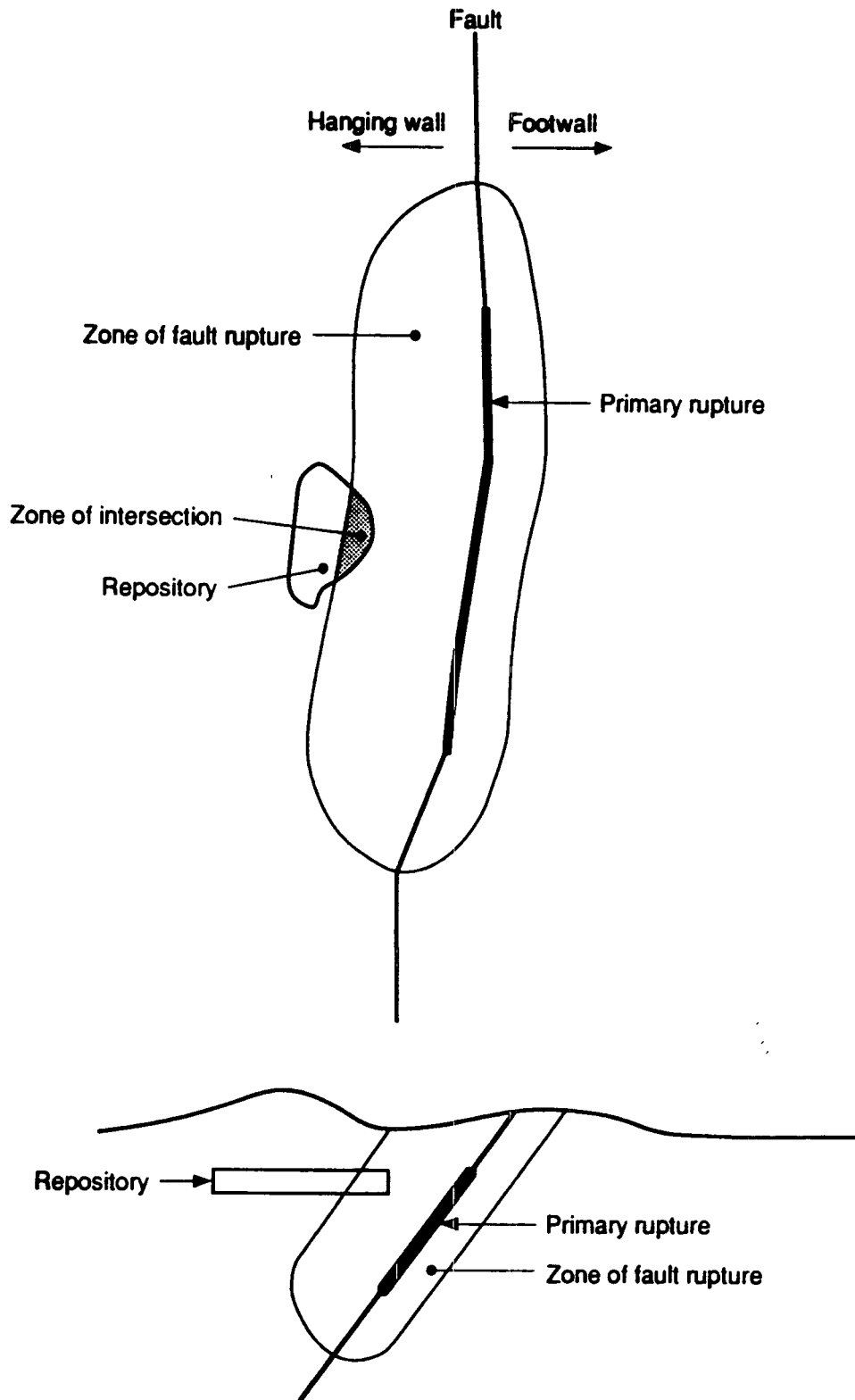


*De Polo et al., 1990*

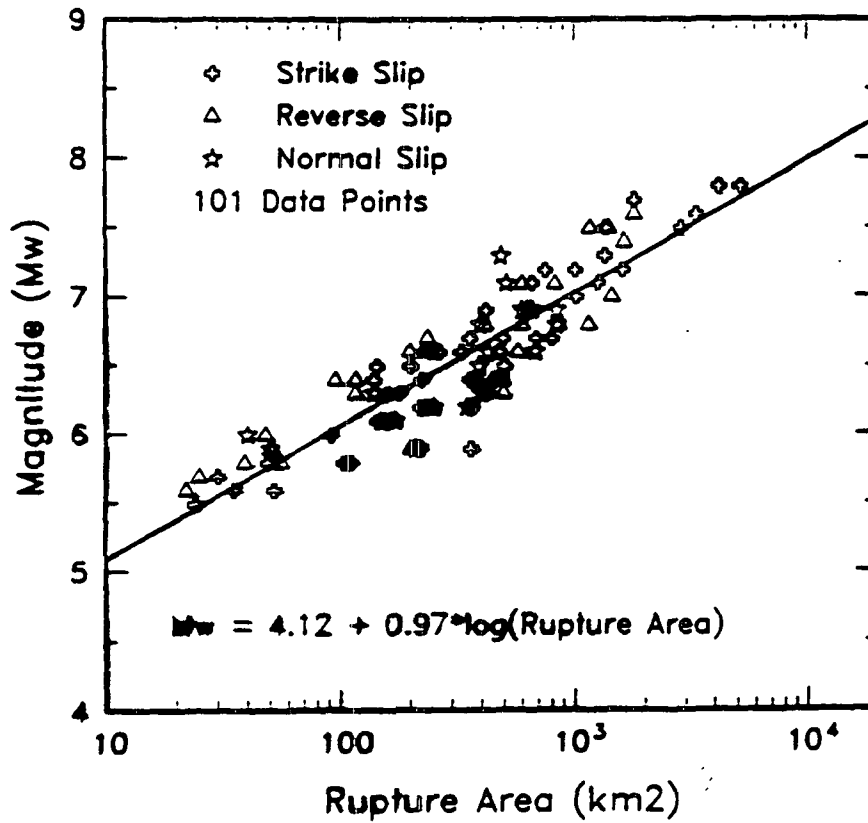
Figure 4. 1915 Pleasant Valley (from Wallace, 1984), CM=China Mountain scarp, P=Pearroe scarp, S=Stillwater scarp, SH=Sou Hills scarp, T=Tobin scarp.

Figure 5. 1932 Cedar Mountain (from Gianella and Callegnan, 1934), GV=Gabbs Valley, MCV=Monte Cristo Valley, SV=Stewart Valley.

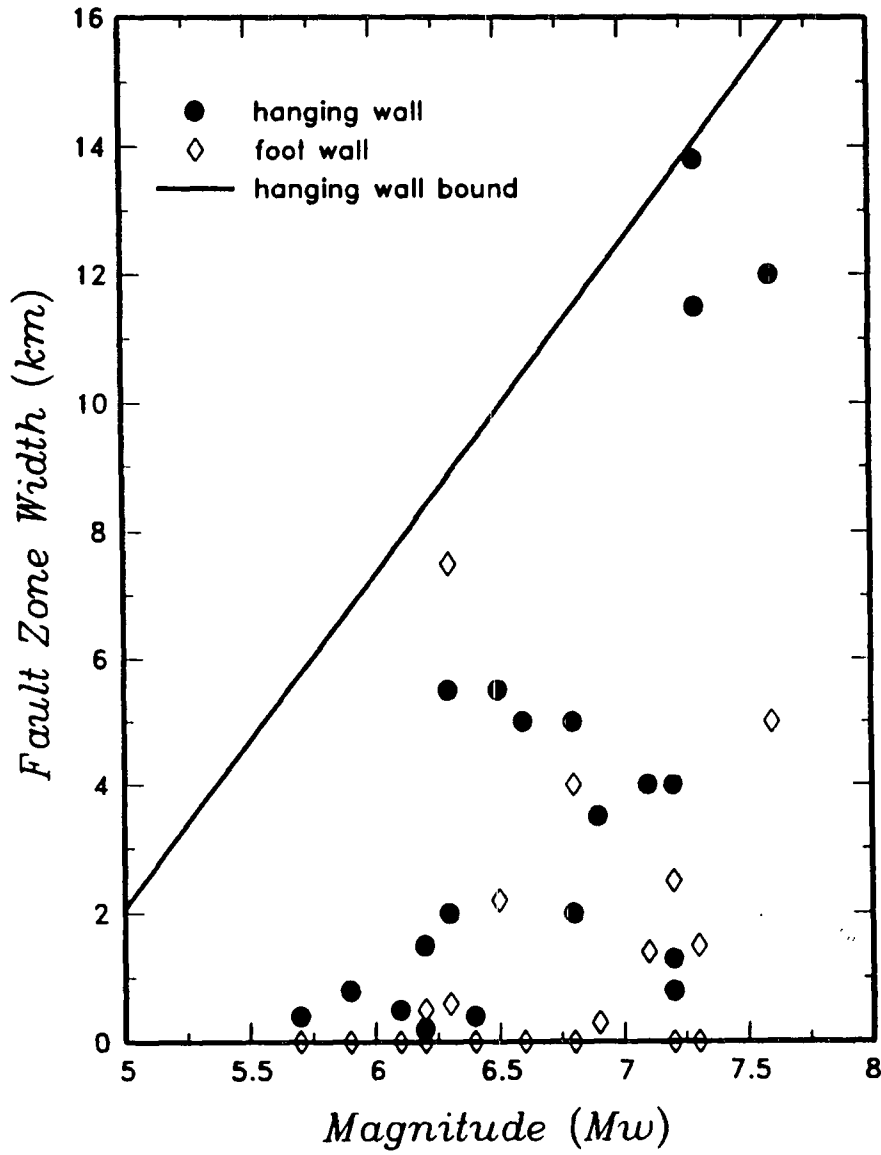


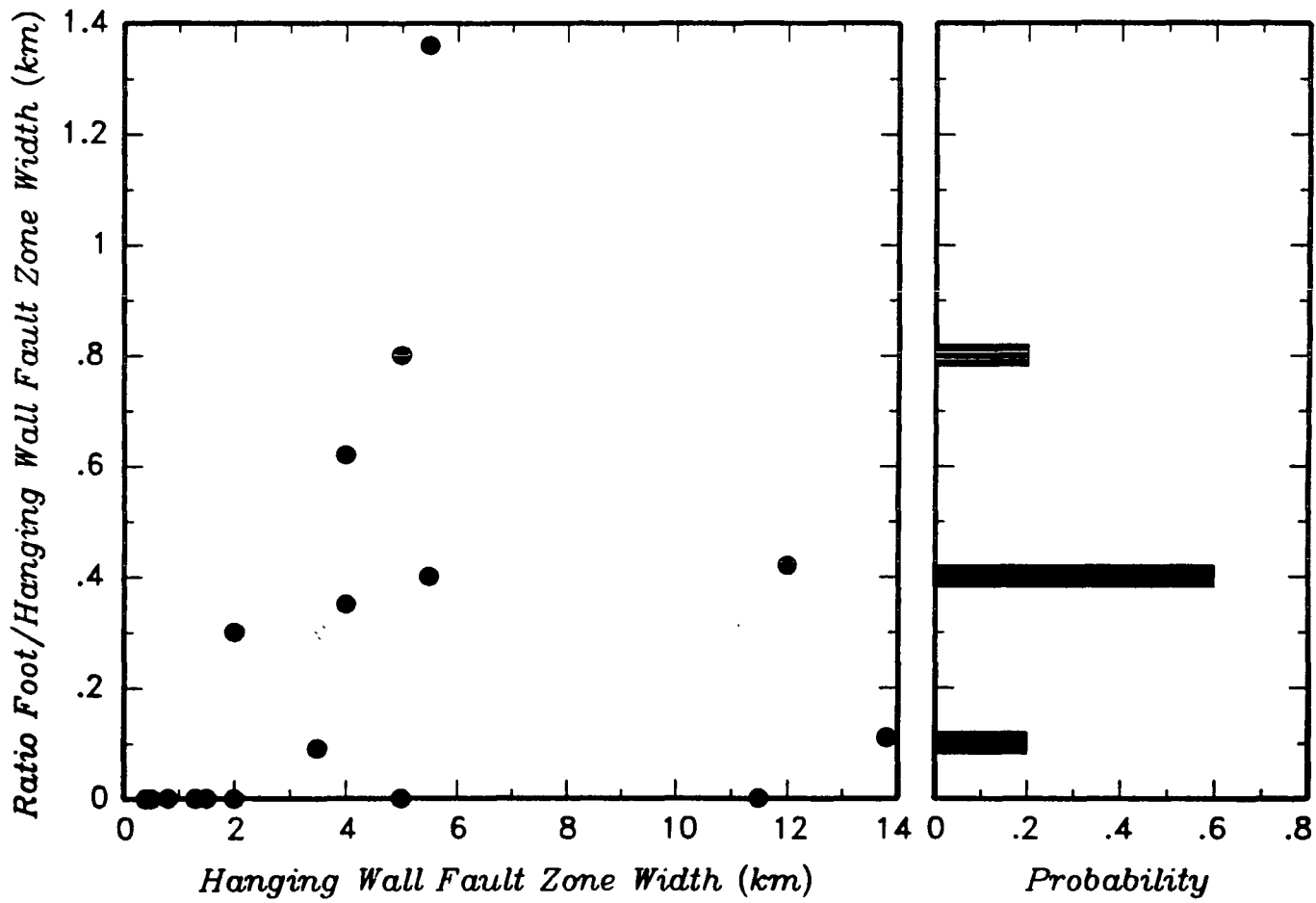


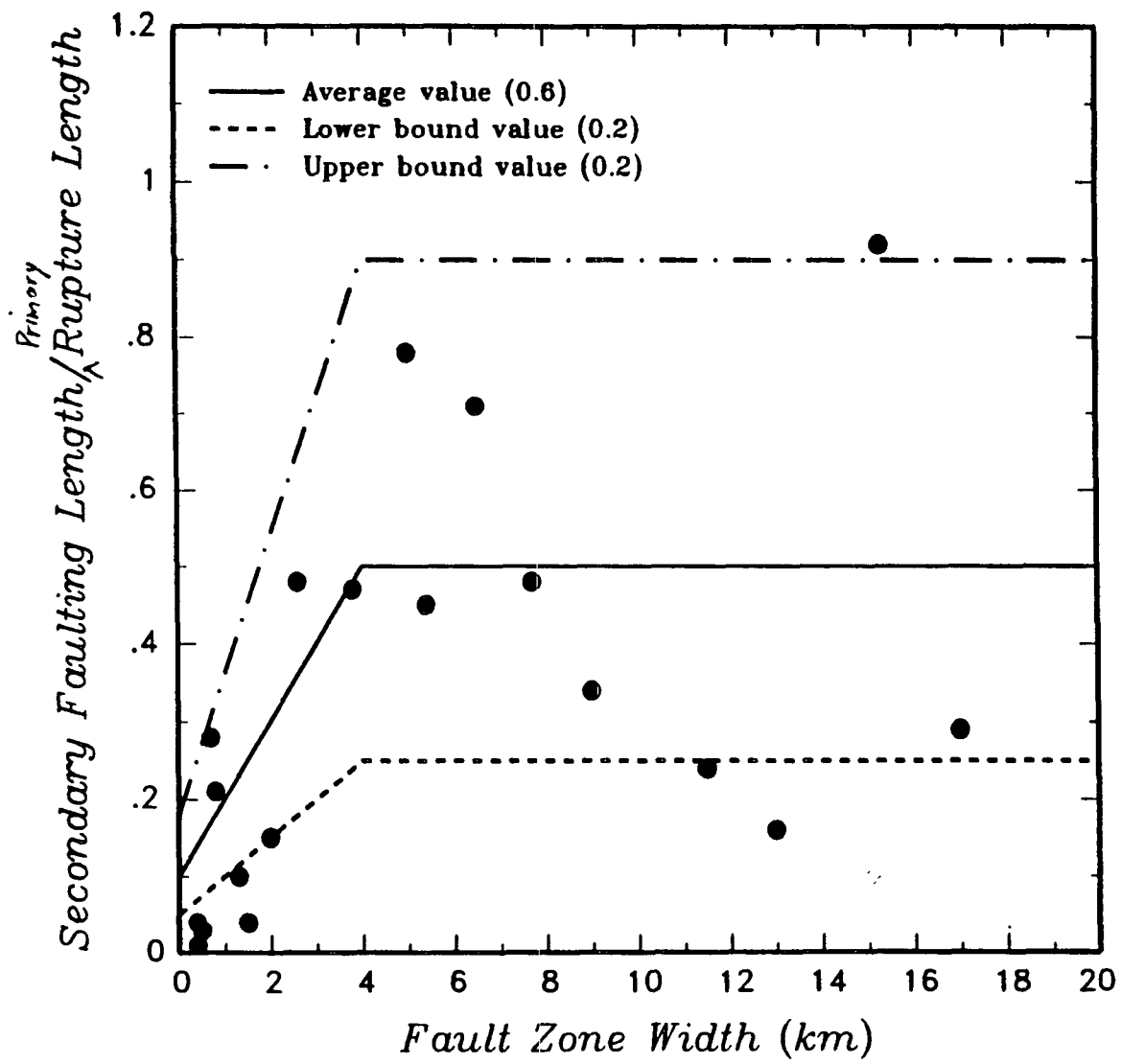
## Magnitude Mw vs. Rupture Area

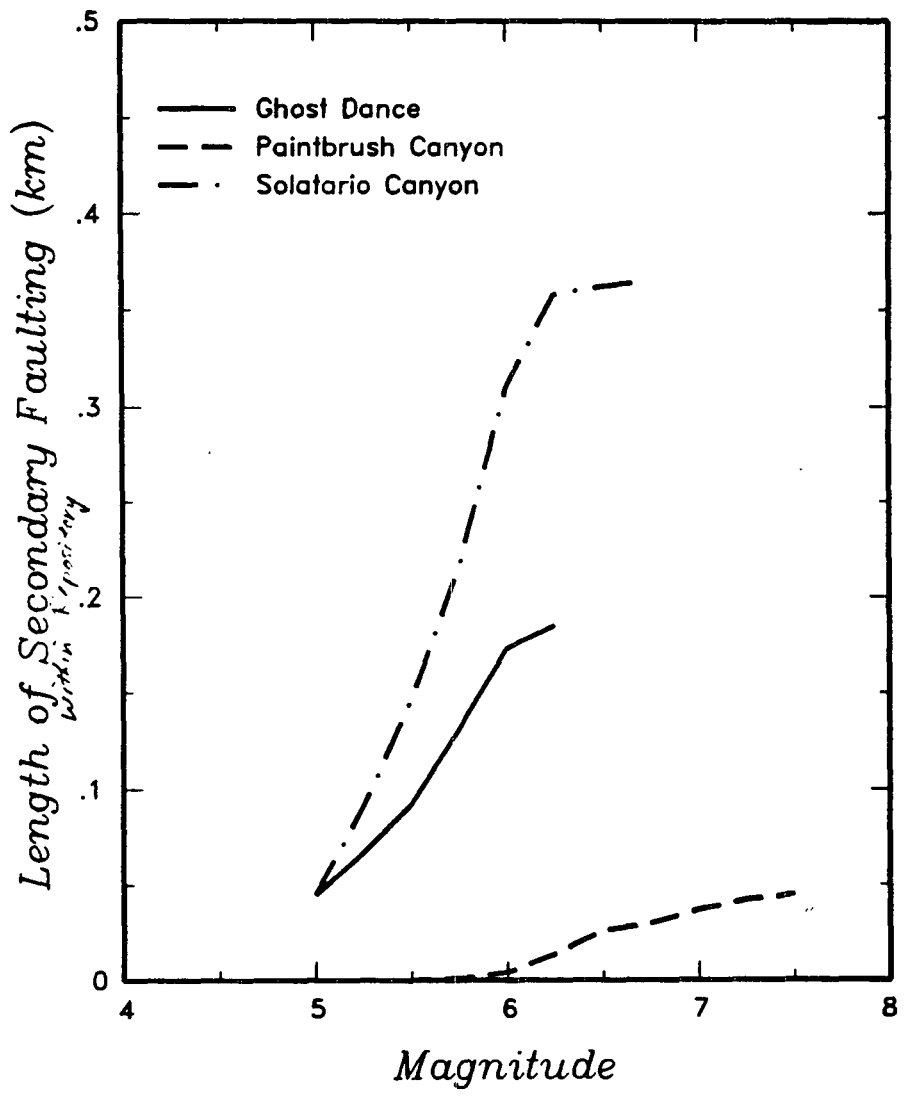


Wells and Coppersmith, (in preparation)

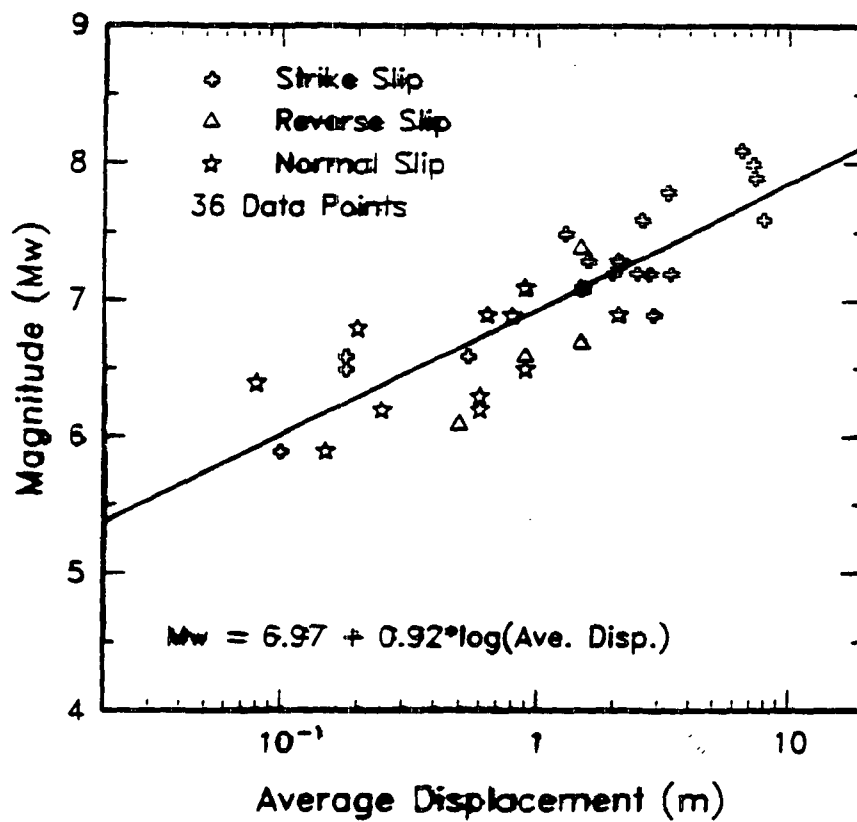




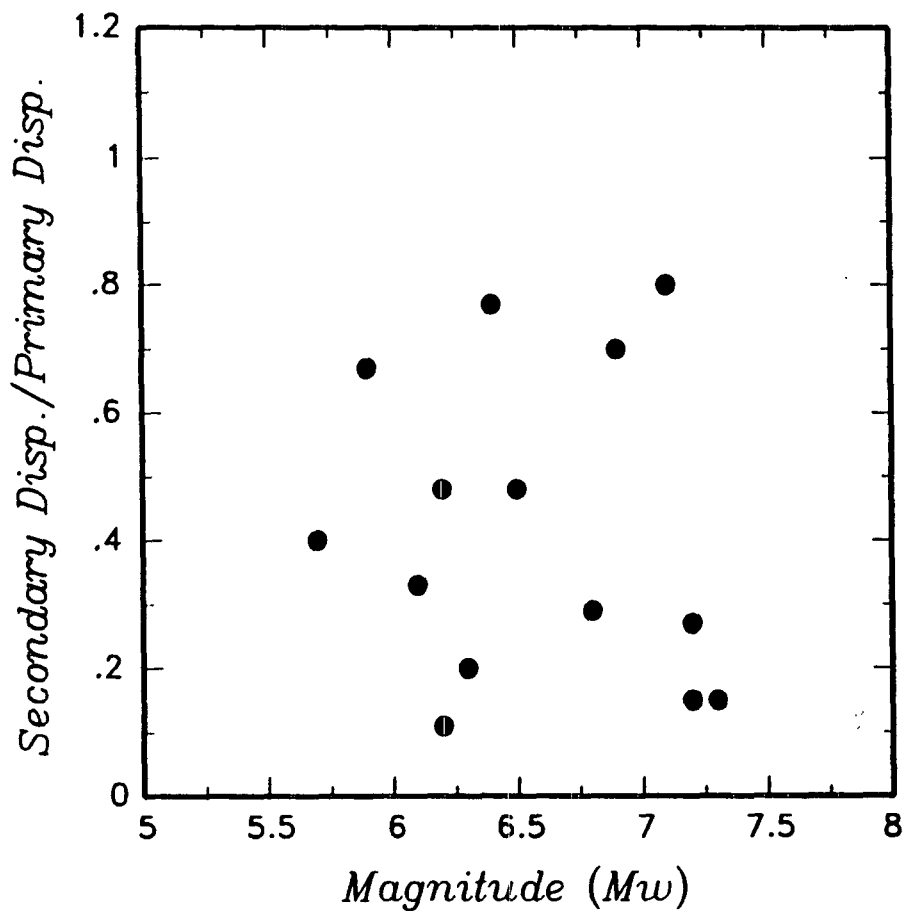




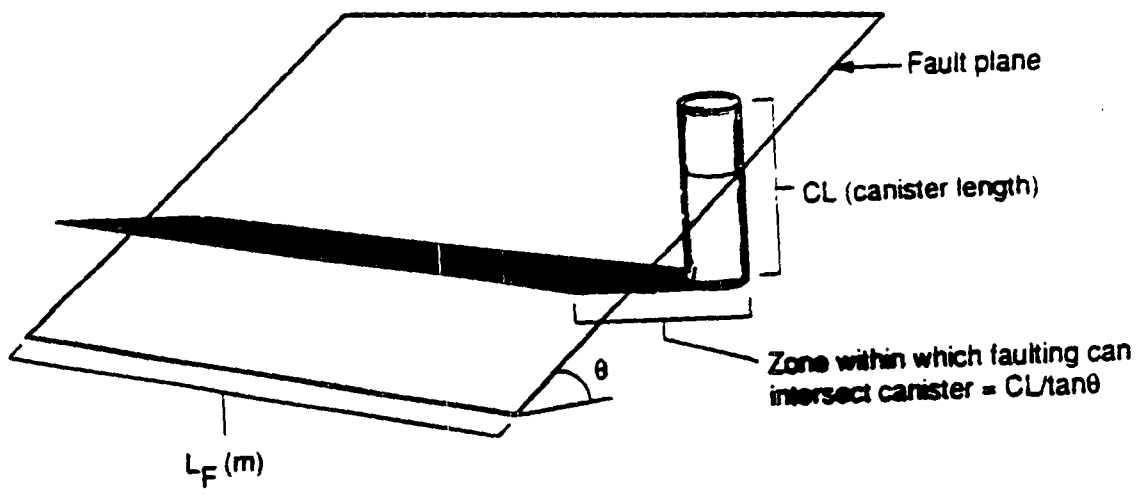
## Magnitude Mw vs. Average Displacement

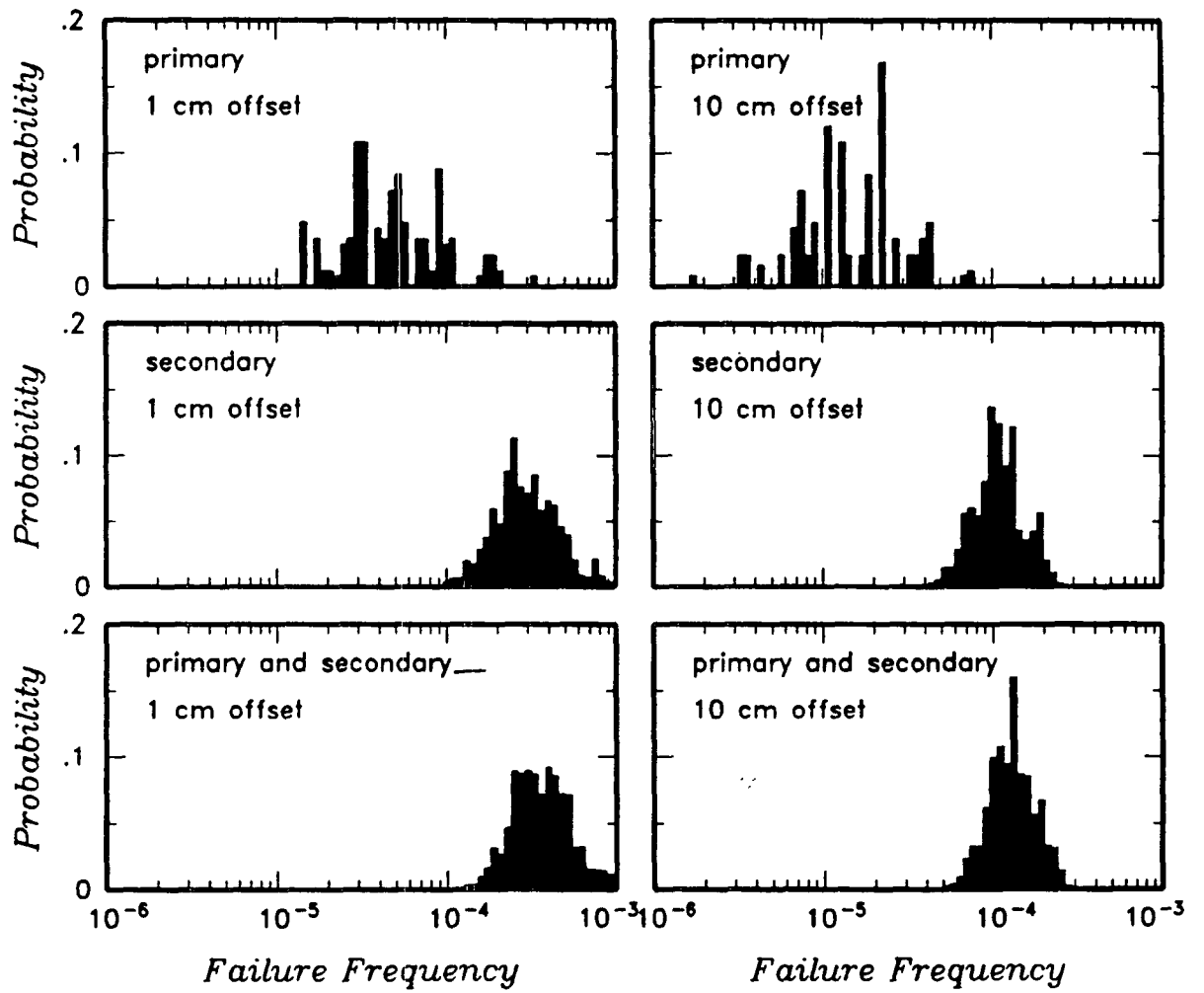


Wells and Coppersmith, (in preparation)









# **EPRI-HLW WORKSHOPS ON EARTHQUAKES AND TECTONICS**

**November 14-15, 1991  
March 4-6, 1992**

## **Objectives**

- **To demonstrate elicitation of expert judgement**
- **To quantify the uncertainties associated with earthquake and tectonics issues for use in HLW performance assessment models**

## **QUANTIFICATION OF UNCERTAINTY**

**The focus of the EPRI-HLW performance assessment methodology is the quantification of uncertainties in the various components leading to the probability of radionuclide release in 10,000 years.**

- Description and proper quantification of uncertainties is an essential part of any performance assessment**
- Single-valued parameters imply either perfect knowledge or unrealistically narrow range of possible values**
- One effective means of quantifying uncertainty is through the elicitation of expert opinion**
- Each expert can assign range of uncertainty in his own assessments**
- Multiple experts can express diversity of opinions**

# **SELECTION OF THE EXPERT PANEL**

## **PURPOSE OF THE PANEL**

- 1. To quantify the uncertainties associated with earthquake and tectonics issues for the performance assessment model.**
- 2. To demonstrate methodologies for eliciting expert judgements for uncertainty treatment**

## **GUIDELINES FOR SELECTION**

- Geologist or seismologist with strong professional reputation and widely recognized competence based on academic training and relevant experience**
- Experience collecting and analyzing research data for relevant studies in the southern Great Basin or similar regions; written documentation of these studies (e.g., in journal articles, technical reports, etc.)**
- Ability and willingness to participate**
- Panel balanced to contain individuals with diverse opinions, areas of technical expertise, and institutional/organizational backgrounds (e.g., government agencies, academic institutions, and private industry)**

## **CONCLUSIONS**

- **Panel represents a balanced group. It is quite likely that other individuals could be identified with equivalent skills and backgrounds**
- **We are interested in each expert's personal judgements-- not representing positions taken by their organizations**

# **NORMATIVE EXPERTS**

## **EPRI-HLW PROJECT**

**The role of the normative experts in the EPRI-HLW project is to train the earthquakes and tectonics experts, to guide and assist in the individual elicitations of expert judgements, and to provide guidance regarding the methodologies for aggregating the expert judgements.**

**Ralph Keeney**

**University of Southern California**

**Detlof Von Winterfeldt**

**University of Southern California**

**Robert Winkler**

**Duke University**

# **SCHEDULE FOR EARTHQUAKES AND TECTONICS**

## **EPRI-HLW PROJECT**

**The milestones for the quantification of uncertainties on earthquakes and tectonics for the EPRI-HLW project consist of the following:**

<b><u>Milestone</u></b>	<b><u>Date</u></b>
<b>Distribution of data package and pertinent references</b>	<b>October, 1991</b>
<b>November Workshop: data and preliminary technical issues, elicitation training</b>	<b>November 14-15, 1991</b>
<b>Sample elicitation</b>	<b>February, 1992</b>
<b>Analysis of issues (models and data), distribution to panel members</b>	<b>Dec., 1991 - Feb., 1992;</b>
<b>March Workshop: discussion of models, data, individual elicitation, feedback</b>	<b>March 4-6, 1992</b>
<b>Review of elicitation documentation</b>	<b>April-May, 1992</b>
<b>Production of final report</b>	<b>September, 1992</b>



**MODELING FAULT RUPTURE HAZARD  
FOR THE PROPOSED REPOSITORY AT YUCCA MOUNTAIN, NEVADA**

K.J. Coppersmith and R.R. Youngs, Geomatrix Consultants  
100 Pine St., Suite 1000  
San Francisco, California 94111  
415/434-9400

**ABSTRACT**

As part of the Electric Power Research Institute's High Level Waste program, we have developed a preliminary probabilistic model for assessing the hazard of fault rupture to the proposed high level waste repository at Yucca Mountain. The model is composed of two parts: (1) the earthquake occurrence model that describes the three-dimensional geometry of earthquake sources and the earthquake recurrence characteristics for all sources in the site vicinity; and (2) the rupture model that describes the probability of coseismic fault rupture of various lengths and amounts of displacement within the repository horizon 350 m below the surface. The latter uses empirical data from normal-faulting earthquakes to relate the rupture dimensions and fault displacement amounts to the magnitude of the earthquake. Using a simulation procedure, we allow for earthquake occurrence on all of the earthquake sources in the site vicinity, model the location and displacement due to primary faults, and model the occurrence of secondary faulting in conjunction with primary faulting. The probability of various lengths of fault intersection with the proposed repository and the amount of slip provides the expression of the fault rupture hazard. Our preliminary results show that the frequency of earthquake-induced canister failure is on the order of  $10^{-4}$  per year. Importantly, it is also found that the largest contribution to the fault displacement hazard comes from secondary faulting, rather than primary faulting.

**INTRODUCTION**

This paper presents a model for addressing the hazard posed by fault rupture to the proposed high level waste repository at Yucca Mountain, Nevada. This model is part of a performance assessment methodology developed by the Electric Power Research Institute.<sup>1</sup> Specifically, we address canister failure caused by offset of the canister boreholes due to fault slip on recognized primary faults and along minor or unrecognized faults. Fault rupture through the repository horizon is considered to be the primary earthquake hazard to the repository's post-closure performance. A secondary effect of earthquake occurrence may be a coseismic rise in the water table associated with changes in the local stress field. This effect has also been modeled in other parts of EPRI's performance methodology development.<sup>1</sup> Strong vibratory ground motions, while undoubtedly an important consideration for the surface facilities, are considered to have little potential effect on the canisters within the repository during the post-closure period.

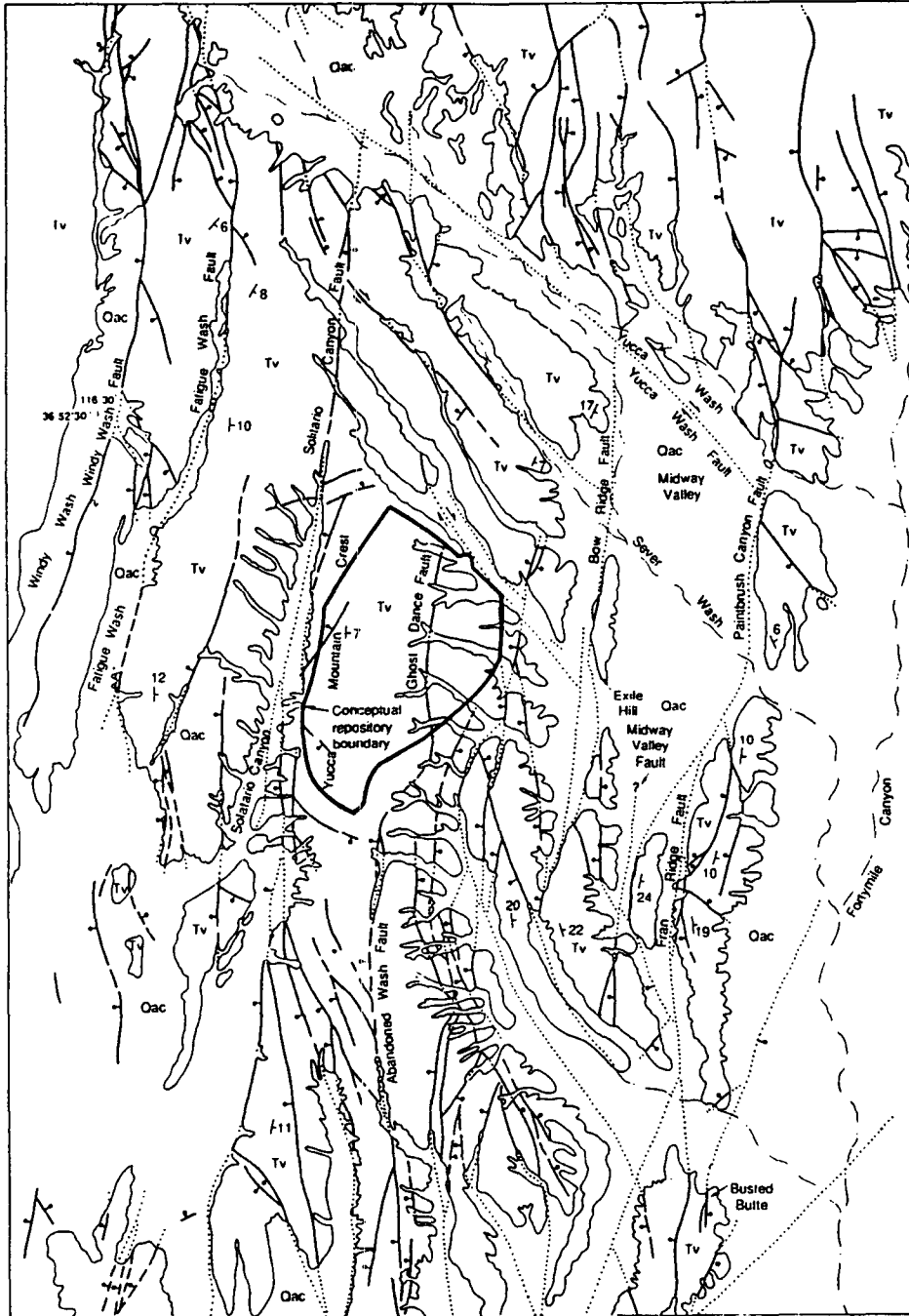
This model provides a general framework and methodology for modeling the fault displacement hazard at Yucca Mountain. The ongoing EPRI program is quantifying the uncertainties in the fault displacement hazard using the assessments of multiple experts.

The model developed in this paper builds on the general formulation for probabilistic seismic hazard assessment, first outlined by Cornell.<sup>2</sup> The model consists of two parts: (1) a seismic source model that defines the location, size, and frequency of earthquakes, and (2) a fault rupture model that simulates primary and secondary ruptures in three-dimensions to define the distributions for length of faulting through the repository and amount of fault displacement. Part (1) represents the standard seismic source characterization that would be performed for a probabilistic assessment of ground motion hazard. We have utilized the advances in probabilistic characterization of seismic sources described in Coppersmith.<sup>3</sup> Part (2) represents the major focus of this paper—development of a model of the spatial distribution of rupture associated with a normal-faulting event. Our model is based on simple probability models parameterized using empirical observations of surface faulting during normal-faulting earthquakes. Each of the two parts of the model are discussed below.

**EARTHQUAKE SOURCE MODEL**

Figure 1 shows the location of the faults that have been mapped or inferred to lie in the vicinity of the proposed repository. The faults selected are those that lie within about one down-dip fault width (about 15 - 20 km) from the repository. The location and orientation prescribed to the selected faults are based on available geologic mapping. The late Quaternary-Holocene behavior of most of the faults is not very well known and, in many cases, the locations of the fault is based on exposures within Tertiary volcanic units. In some regions, such as within the Midway Valley area, faults have been inferred but have not yet been either imaged using geophysical data or directly observed in exploratory trenches, although such studies are underway.

For this study, we assume that the named faults identified in Figure 1 are "primary" faults in that they exhibit the largest amounts of cumulative displacement and have, in the geologic past, been the locus of most of the coseismic slip. As discussed



Geology compiled from Scott and Bank (1984), Maldonado (1985) and Swadley and Parrish (1988);  
 conceptual repository boundary from Holmes and Narver (1988).

EXPLANATION

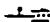
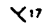
- Oac (Quaternary) Alluvium and Colluvium
- Tv (Tertiary) Siltic Volcanic Rocks
-  Fault - dotted where concealed; ball and bar on downthrown side; arrows indicate relative movement
-  Strike and dip of bedding or foliation



Figure 1. Location map of faults considered in assessment of potential fault rupture in repository.

later, we assume that secondary faults occur randomly within a zone surrounding the primary faults. The scattered pattern of minor faults seen in the volcanic bedrock in the vicinity of the primary faults supports our assumption of a random secondary fault pattern.

Each fault was characterized in terms of its activity, geometry, maximum magnitude, frequency of earthquake generation, and earthquake size distribution. Uncertainty regarding these parameters was incorporated into the analysis through the use of logic trees. The logic tree formulation for seismic hazard analysis involves specifying discrete alternatives for states of nature or parameter values and specifying the relative likelihood that each discrete alternative is the correct value or state of the input parameter.<sup>4, 5, 6, 7</sup> Figure 2 shows the logic tree used to model the uncertainty in the source characterization parameters for the Ghost Dance fault. Similar logic trees were constructed for the other faults shown in Figure 1. The various parameters represented in the logic trees are briefly discussed below.

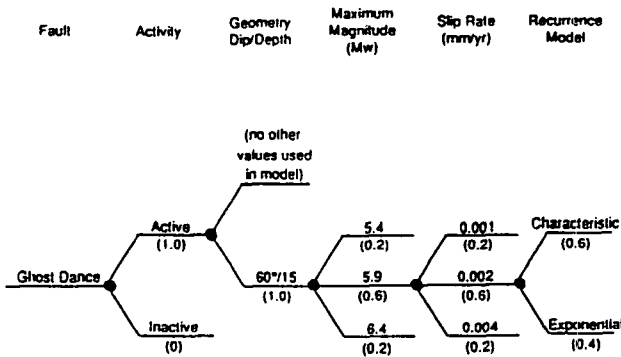


Figure 2. Earthquake logic tree for Ghost Dance fault.

### Fault Activity

An active fault is defined as one that has the potential to undergo slip and generate earthquakes within the present tectonic environment. Studies of the tectonics and contemporary stress regime in the Yucca Mountain are not complete, but they suggest that, east of the Furnace Creek fault zone, the region is characterized by regional northeasterly-directed extension. The sense of slip derived from instrumental focal mechanisms of earthquakes shows both normal-faulting and extensional strike-slip faulting. These considerations of the stress regime are used, as well as the sparse available data regarding recency of faulting to make assessments of the probability that individual faults are active. It is assumed that the regional tectonic regime will not change over the lifetime of the repository.

### Fault Geometry

The geometries of all faults are modeled in three dimensions in order to realistically portray the possibility of fault displacements intersecting the repository, and as a means of

assessing fault parameters related to the dimensions of faults, such as maximum magnitudes and seismic moment rate. At the present time fault-specific data do not exist to directly characterize the geometries of the particular faults in the repository vicinity. In-lieu of fault-specific data, we rely on average fault characteristics determined for a large number of Basin and Range earthquakes by Doser and Smith.<sup>8</sup> The Doser and Smith compilation indicates that a dip angle of about 60 degrees and a focal depth of about 15 km is typical for Basin and Range faulting events. These values have been adopted for the present application.

### Maximum Earthquake Magnitude

None of the faults considered in this analysis has generated a significant moderate to large earthquake within the historical record, demanding that means other than the historical seismicity record be used to estimate the maximum earthquake possible on each fault. Therefore the geometry of expected fault ruptures is used to estimate maximum magnitudes. This approach has become standard for maximum magnitude estimation in the western United States.<sup>9</sup> Typically, maximum magnitudes are assessed on the basis of estimates of the rupture length, rupture area, and displacement per event, as determined from geologic studies of the individual faults. Fault-specific studies of this type have not yet been carried out in the Yucca Mountain vicinity. For this analysis, we estimated maximum magnitudes on the basis of well-constrained relationships between fault rupture area and magnitude,<sup>10</sup> assuming that the faults as mapped will rupture segments of their length and that their downdip rupture geometry is as defined above. In the earthquake logic tree (Figure 2) these estimates are used as the preferred values and an uncertainty of plus-or-minus one-half magnitude unit was assumed in each estimate.

### Fault Slip Rate

The basic fault displacement model is probabilistic, therefore, the frequency of occurrence of earthquakes of various sizes on each fault must be specified. Because the historical seismicity is insufficient to establish such fault-specific recurrence, fault slip rate is used to estimate average recurrence.<sup>11, 12</sup> It is assumed that all of the slip accumulated on the fault and represented by displacement of units of various ages is representative of seismogenic slip and has not occurred by aseismic processes.

At the time this model was developed, slip rates have only been estimated for the Paintbrush Canyon and Bow Ridge faults,<sup>13</sup> and even for these the data are sparse relative to other known faults, particularly in terms of the constraints on rates in the past one million years. In any case, the rates of Gibson and others have been adopted for the Paintbrush Canyon and Bow Ridge faults. They suggest that the rate of slip along these faults have decreased significantly from about 0.035 mm/yr during the period about 8-13 my ago to about 0.006 mm/y averaged over the past 8 my and attribute this decrease in slip rate to a change in the tectonic environment from one of active caldera formation and associated silicic volcanism to one of simply regional extension and minor basaltic volcanism. The rates for the remaining faults have been estimated based on the relative amounts of cumulative displacement of the 13 million year old

Paintbrush Tuff unit compared to those measured for the Paintbrush and Bow Ridge faults.

### Earthquake Recurrence Model

The fault slip rate is used together with the geometry of the fault to define the seismic moment release rate along the fault zone. Seismic moment, which is directly correlated with to earthquake magnitude, is thereby expressed per unit time. In order to develop a recurrence relationship between frequency of occurrence and earthquake magnitude, the seismic moment rate must be partitioned into earthquakes of various magnitude up to the maximum for the fault of interest according to a particular recurrence (size distribution) model. The characteristic earthquake model<sup>12</sup> and truncated exponential recurrence models have been considered and a greater weight has been given to the characteristic model for defining the recurrence distribution for individual faults.

### Predicted Earthquake Recurrence Rates

The end branches of the earthquake source logic tree for each fault define a discrete distribution for the parameters necessary to describe the spatial and temporal occurrence of various size earthquakes on the faults in the vicinity of the repository. For example, an earthquake recurrence relationship can be computed for each end branch of the logic tree for a fault. By averaging the resulting recurrence relationships over all end branches of the earthquake logic tree, the expected or average earthquake recurrence relationship for the fault is obtained. The resulting average earthquake recurrence relationships developed for each fault are shown in Figure 3.

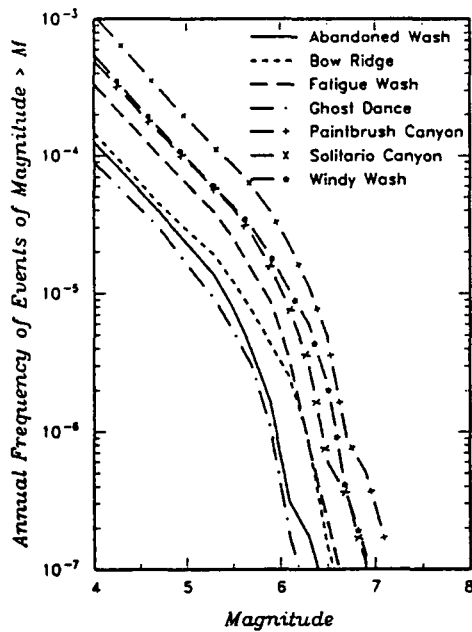


Figure 3. Predicted earthquake recurrence relationships for faults considered in this study.

### FAULT RUPTURE MODEL

The observation of many historical surface fault ruptures indicates that the map-view width of the zone of faulting during an earthquake is often not restricted to a narrow zone along the primary fault, but is often a zone of faulting that is several meters to kilometers wide. The rupture along the coseismic fault is termed "primary" rupture, and the zone of faulting away from the primary fault is termed "secondary" rupture. In the context of the proposed repository, then, there is a consideration of primary and secondary rupture for those faults that actually transect the repository (Ghost Dance fault), and secondary fault rupture related to all faults in the site vicinity.

Figure 4 shows examples of the pattern of surface faulting observed for Basin and Range normal-faulting earthquakes. On the left is the observed surface faulting during the 1915 Pleasant Valley earthquake which exhibited a relatively simple pattern consisting of a narrow zone of primary faulting along the main fault trace with very little secondary rupture. On the right is the pattern of surface faulting observed after the 1932 Cedar Mountain earthquake, which shows a wide and complex zone of secondary rupture. The model developed to estimate the amount of fault rupture that could occur within the repository captures the range of surface faulting patterns observed for Basin and Range earthquakes.

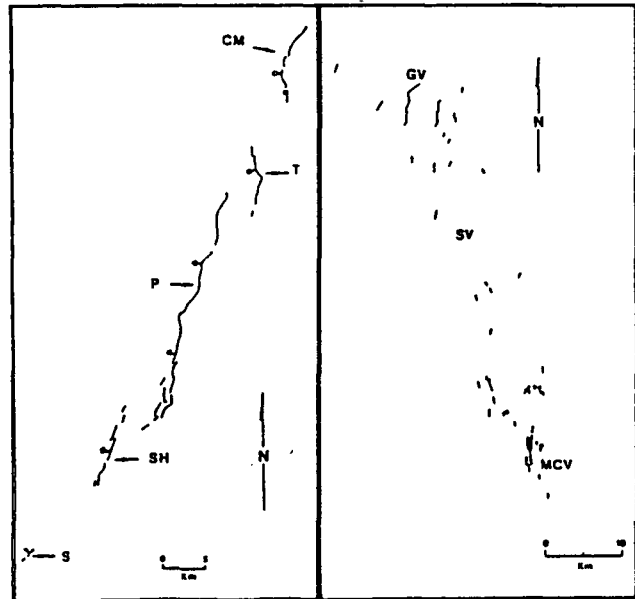


Figure 4. Examples of pattern of surface faulting in Basin and Range normal-faulting earthquakes. On left is the 1915 Pleasant Valley earthquake and on right is the 1932 Cedar Mountain earthquake.

The fault rupture model we have developed attempts to capture the diversity of behavior shown in Figure 4. Planned geologic studies in the Yucca Mountain vicinity, as well as mapping of faults during the excavation of the repository itself, may allow a fault-specific consideration of individual secondary

fault. For now, however, because we lack knowledge about the complexity of past ruptures on the faults in the site vicinity, we have relied on empirical distributions of fault rupture behavior observed in other normal-faulting earthquake ruptures to define the characteristics of potential future fault ruptures in the vicinity of the proposed repository. These distributions are based on review of twenty historical ruptures that have been well documented in the published literature. From these data we have developed distributions for the width of the zone of faulting, the total length of secondary faulting, and the amount of secondary fault slip as a function of the dimensions of the primary rupture. Through a simulation process, we randomly select parameters from these distributions to construct scenarios of future fault ruptures. The statistics of the length and amount of fault offset intersecting the proposed repository are then used to estimate the potential hazard, given a specific size rupture on the fault. The dimensions of the primary rupture are specified as a function of the magnitude of the future earthquake and are given by empirical relationships developed from a much larger data set by Wells and Coppersmith.<sup>10</sup> The secondary faulting parameters are discussed below.

### Width of Zone of Faulting

The data gathered for this study show that the width in map view of the zone of faulting during normal-faulting earthquakes varies from essentially zero to as much as 14 km. Figure 5 shows the data for both the hanging wall and foot wall sides of the zone. The hanging wall side of the fault zone is typically where much of the secondary faulting occurs. The data show no significant correlation with magnitude, although the largest observed width does increase with earthquake magnitude. One would expect that the maximum width of the zone of faulting should increase as the primary down-dip width of faulting increases, and thus increase with increasing magnitude. We have assumed that an upper bound to the half-width of zone of faulting on the hanging wall side can be represented by the solid line shown in Figure 5. The bound to the data was drawn to provide a significant potential width for magnitude 5 earthquake ruptures. We assume that the hanging wall fault zone half-width in any randomly selected future rupture is uniformly distributed between zero and the bounding line shown in Figure 5.

Figure 6 shows the ratio of foot wall to hanging wall fault zone half-width plotted against hanging wall half-width. As can be seen, there is little correlation between this ratio and the hanging wall fault zone half-width. Therefore, the discrete distribution shown on the right in Figure 6 was assumed to apply to all potential ruptures.

### Length of Secondary Faulting

The zone of surface faulting can contain a single strand of secondary faulting, or multiple strands. Lacking detailed knowledge of the distribution of rupture for past earthquakes on the faults in the site vicinity, we first estimate the total length of secondary faulting that may occur in an earthquake and then distribute that length over the area defined by the zone of faulting. The best correlation found in the data was between the ratio of the length of secondary faulting to the length of primary faulting,  $R_{SP}$ , and the maximum width of the zone of faulting. Figure 7 shows  $R_{SP}$  plotted against the fault zone width. As can

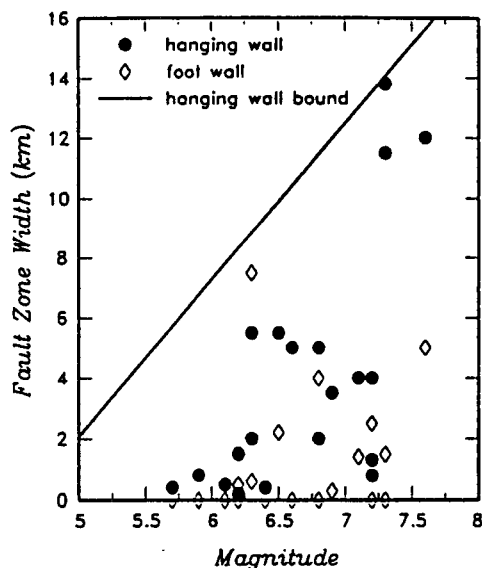


Figure 5. Maximum width of zone of faulting, measured from primary fault trace, versus earthquake magnitude for normal-faulting events. Shown also is the assumed bound on hanging wall fault zone width.

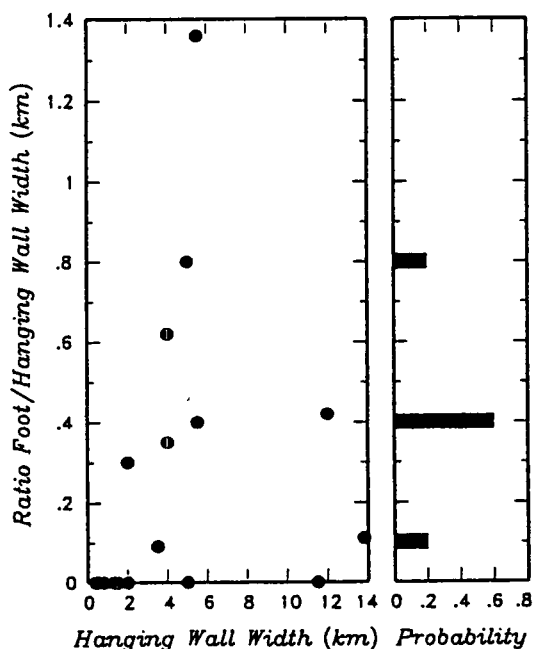


Figure 6. Ratio of foot wall/hanging wall fault zone width (measured from primary rupture trace) for data shown in Figure 5. Left hand plot shows the reported data, the right hand plot shows the discrete distribution used in the simulations.

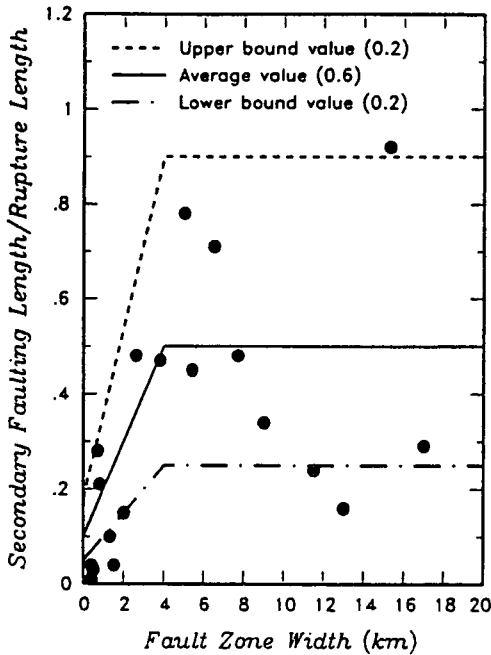


Figure 7. Ratio of total length of secondary faulting to total length of primary faulting,  $R_{SP}$ , versus maximum width of zone of faulting. The three lines show the weighted relationships used in the simulations.

be seen, there is considerable scatter in the data and, once the fault zone has significant width, the ratio  $R_{SP}$  does not show asystematic increase with increasing width. We have assumed that the variability in the total length of secondary faulting can be modeled by a three point discrete distribution defined by the three relationships indicated in Figure 7.

#### Estimation of the Length of Faulting within the Repository

The length of faulting within the repository, given the occurrence of an earthquake on a fault, was evaluated using the simulation procedure illustrated schematically in Figure 8. Given a magnitude  $m$  earthquake, the down-dip width and length of primary faulting were computed from an empirical relationship between primary rupture area and magnitude.<sup>10</sup> The primary rupture area is then randomly located on the fault plane assuming all locations are equally likely. The hanging wall fault zone half-width in map view of the zone of faulting is then randomly selected from a uniform distribution between zero and the bound to the data shown in Figure 5. The ratio of foot wall/hanging wall half-width is then selected from the discrete distribution shown on the right in Figure 6. The two half-widths are then used to construct a zone of faulting around the primary rupture plane, as shown in Figure 8.

The fraction of the total area of the zone of faulting that falls within the repository boundary,  $F_{RI}$ , is then computed. Assuming that secondary fault rupture is equally likely to occur anywhere within the zone of rupture, then the fraction of the

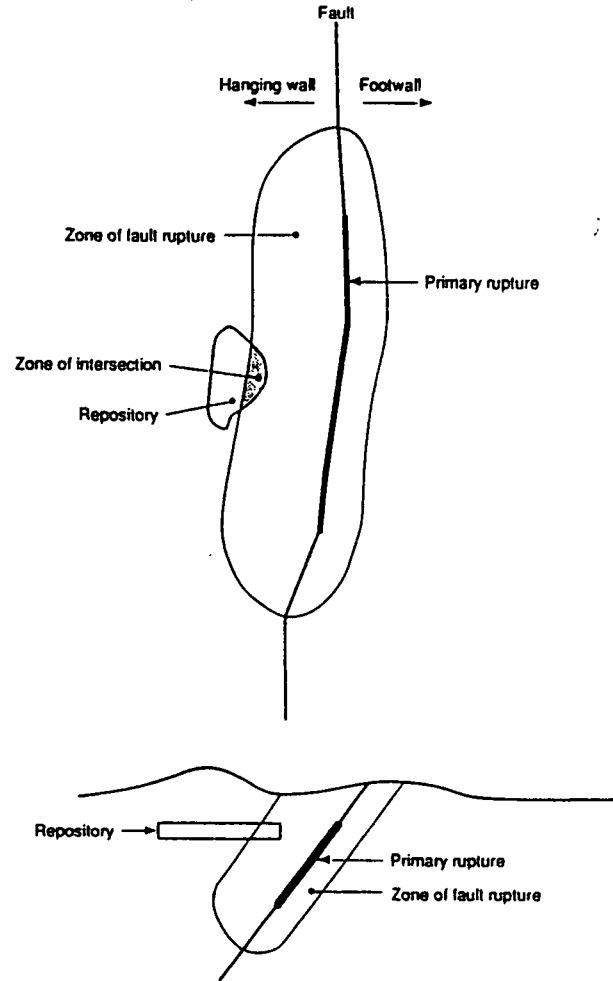


Figure 8. Illustration of simulation of a zone of faulting for a single event occurring on a fault near the repository. Shaded area represents the area of intersection of the rupture zone with the repository footprint.

total length of secondary rupture that is expected to occur within the repository is equal to the fraction of the total area of the zone of faulting that falls within the repository boundary,  $F_{RI}$ . The total length of secondary faulting as a percentage of the length of primary faulting,  $R_{SP}$ , is selected from the weighted relationships shown in Figure 7 and the selected half-width of the zone of faulting. The expected length of secondary faulting in the repository for simulation  $i$ ,  $L_{SF}(m)_i$ , is given by

$$L_{SF}(m)_i = F_{RI} \cdot R_{SP_i} \cdot L_R(m) \quad (1)$$

where  $L_R(m)$  is the length of primary fault rupture on the fault plane.

The simulation is then repeated, selecting a new location on the fault plane for the primary rupture and new values of the half-width of the zone of faulting and length of secondary faulting. In this process, if the primary rupture does not extend

upward to a depth within a rupture zone half-width below the repository depth, then no intersection with the repository is assumed to occur for that simulation. Averaging over all simulations provides an estimate of the expected length of secondary faulting within the repository for a given magnitude earthquake on a given fault,  $E[L_{SF}(m)]_n$ .

The above process was repeated for all magnitudes that could occur on the particular fault, and for all faults considered in the analysis. Figure 9 shows typical results for the relationship between earthquake magnitude and the expected length of secondary fault rupture within the repository. The value of  $E[L_{SF}(m)]_n$  begins to level off with increasing magnitude for the faults very near the repository because the larger ruptures produce fault zones that extend well beyond the repository. In addition, the length of secondary faulting is increasing proportionally to the length of primary faulting, while the fault zone area is increasing proportionally with the square of the length of primary faulting. In our model, this results in a tendency for reduction in the length of secondary faulting per unit area of the zone of faulting for the larger magnitude events.

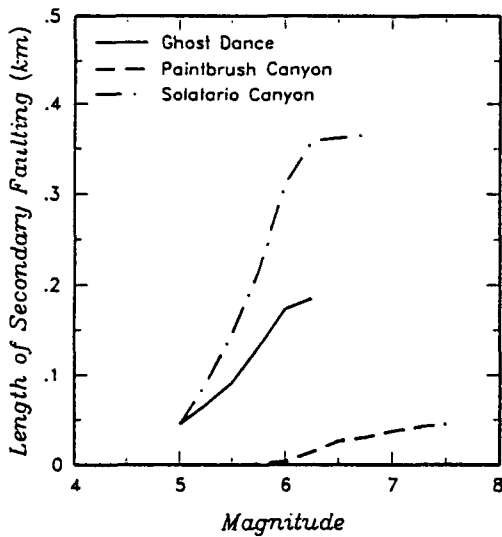


Figure 9. Typical computed relationships between earthquake magnitude and the expected length of secondary faulting within the repository.

The length of primary fault rupture within the repository was assessed using the same procedure. For primary faulting the fault zone width was set to near zero (only faults that pass through the repository contribute to the primary rupture hazard) and the ratio  $R_{SF}$  was set to unity.

#### Amount of Fault Slip

The amount of primary fault displacement occurring in a given magnitude earthquake is typically modeled as lognormally distributed about a median value that depends linearly on earthquake magnitude. We used the empirical relationship between magnitude and average fault slip developed by Wells and Coppersmith.<sup>10</sup> The amount of secondary faulting

displacement is typically a fraction of the amount of primary faulting displacement. Examination of the data for normal-faulting earthquakes indicates that the ratio of secondary faulting displacement to primary faulting displacement can be as high as 0.8 and shows no significant correlation with earthquake magnitude or other faulting parameters. For this analysis we assumed that the ratio of secondary to primary displacement for a randomly selected future earthquake is uniformly distributed between 0.0 and 0.8.

### FAULT RUPTURE HAZARD MODEL

#### Model Formulation

In the EPRI performance assessment methodology fault rupture hazard is represented by the frequency of earthquake-induced canister failure,  $\nu_{CF}$ . The failure rate is computed by

$$\nu_{CF} = \sum_n \alpha_n(m^o) \int_m f(m)_n \cdot E[N_{CF}(m)]_n dm \quad (2)$$

where  $\alpha_n(m^o)$  is the frequency of earthquakes on fault  $n$  with magnitudes greater than a minimum magnitude of interest,  $m^o$ ,  $f(m)_n$  is the density function describing the relative frequency of various magnitude earthquakes, and  $E[N_{CF}(m)]_n$  is the expected number of canister failures in the repository given an earthquake of magnitude  $m$  on fault  $n$ . The parameters  $\alpha_n(m^o)$  and  $f(m)_n$  come directly from the earthquake occurrence model for the faults and are described by the earthquake recurrence curves shown in Figure 3. The parameter  $E[N_{CF}(m)]_n$  is a function of the length of faulting in the repository during an earthquake, the density of canisters within the repository, and the amount of displacement necessary to rupture a waste canister. Assuming vertical canister placement, then the zone over which fault displacements can intersect the waste canister is given by  $L_c / \tan \theta \cdot E[L_F(m)]_n$ , where  $L_c$  is the canister length,  $\theta$  is the fault dip, and  $E[L_F(m)]_n$  is the expected length of faulting (primary or secondary) within the repository given a magnitude  $m$  earthquake. The expected number of canister failures is evaluated by the expression

$$E[N_{CF}(m)]_n = \frac{L_c}{\tan(\theta)} \cdot E[L_F(m)]_n \cdot \frac{35,000}{R_{\text{area}}} \cdot P(D > d_{CF} | m) \quad (3)$$

where  $E[L_F(m)]_n$  is the expected length of faulting in the repository for a magnitude  $m$  earthquake (e.g., Figure 9 for secondary displacement),  $R_{\text{area}}$  is the total area of the repository,  $35,000/R_{\text{area}}$  is the number of canisters per unit area, and  $P(D > d_{CF} | m)$  is the probability that the fault displacement,  $D$ , for a magnitude  $m$  earthquake will exceed the threshold necessary to cause canister failure,  $d_{CF}$ .

#### Example Calculations

For each of the faults shown in Figure 1, Equation 2 was used to compute the frequency of fault displacement-induced canister failure  $\nu_{CF}$  for a given set of earthquake source parameters defined by the end branches of the earthquake logic tree (e.g., Figure 2). The calculation was repeated for all end branches of the earthquake logic tree for each fault, and for all

faults to arrive at a discrete distribution for the frequency of canister failures. For this exercise, the frequency of canister failure was evaluated with  $d_{CF}$  set to 1 and 10 cm. Figure 10 shows the computed distributions for considering only primary rupture (top plots), only secondary rupture (middle plots), and both types of rupture (bottom plots). The average annual probability of canister failure is about  $10^{-4}$  per year. As can be seen, the frequency of canister failure is controlled by the occurrence of secondary rupture.

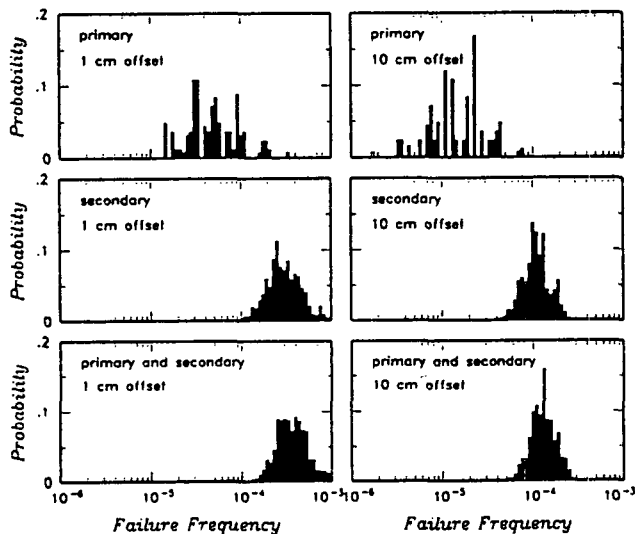


Figure 10. Distribution of annual frequency of canister failure due to faulting within the repository for fault offsets  $d_{CF}$  of 1 and 10 cm. Shown at the top is the effect of primary fault rupture only, in the middle plot is the effect of secondary faulting only, and at the bottom is the combined effects of primary and secondary faulting.

## SUMMARY

We present here a preliminary probabilistic model for assessing the hazard of fault rupture to the proposed high level waste repository at Yucca Mountain. The model consists of a standard probabilistic seismic hazard analysis methodology coupled with a rupture model that describes the probability of coseismic fault rupture of various lengths and amounts of displacement within the repository horizon. We use empirical data from normal-faulting earthquakes to relate the rupture dimensions and fault displacement amounts to the magnitude of the earthquake. Observations of historical surface ruptures in the Basin and Range show that the map pattern of rupture can vary from a relatively simple primary fault trace to a complex pattern of secondary traces surrounding the primary trace, and this range in complexity is incorporated in the EPRI model. We see an indication in the historical data that the map-view width of the fault rupture zone increases with earthquake magnitude and that the ratio of the length of primary rupture to secondary rupture

increases with fault zone width. Using a simulation procedure, we allow for earthquake occurrence on all of the earthquake sources in the site vicinity, model the location and displacement due to primary faults, and model the occurrence of secondary faulting in conjunction with earthquake rupture on the primary faults. The probability of various lengths of fault intersection with the proposed repository and the amount of slip provides the expression of the fault rupture hazard.

Our preliminary results show that the mean frequency of earthquake induced canister failure is on the order of  $10^{-4}$  per year. Importantly, it is also found that the largest contribution to the fault displacement hazard comes from secondary faulting, rather than primary faulting. These preliminary conclusions suggest that a detailed understanding of the behavior and complexity of the faults in the vicinity of the proposed repository should be developed as part of site characterization. Ongoing EPRI studies are quantifying the uncertainties associated with the fault displacement hazard to examine its effect on repository performance. The results are applicable to the other post-closure assessments being undertaken by DOE and its contractors.

## ACKNOWLEDGEMENTS

The work presented in this paper was sponsored by the Electric Power Research Institute under the program management of Dr. Robert A. Shaw. We wish to thank other members of the EPRI High Level Waste Project team for their suggestions and comments and Donald Wells for his efforts in compiling the data base of normal-faulting rupture parameters.

## REFERENCES

1. ELECTRIC POWER RESEARCH INSTITUTE (EPRI), *Demonstration of a Risk-Based Approach to High-Level Waste Repository Evaluation* (1990).
2. C.A. CORNELL, "Engineering Seismic Risk Analysis," *Bulletin of the Seismological Society of America*, 58, 1583-1606 (1968).
3. K.J. COPPERSMITH, "Seismic Source Characterization For Engineering Seismic Hazard Analysis," *Proceedings of the Fourth International Seismic Zonation Conference*, 1, (1991).
4. R.B. KULKARNI, R.R. YOUNGS, and K.J. COPPERSMITH, "Assessment of Confidence Intervals for Results of Seismic Hazard Analysis," *Proceedings of the Eight World Conference on Earthquake Engineering, San Francisco, California*, 1, 263-270 (1984).
5. R.R. YOUNGS, K.J. COPPERSMITH, M.S. POWER and F.H. SWAN III, "Seismic Hazard Assessment of the Hanford Region, Western Washington State," *Proceedings of the DOE Natural Phenomena Hazards Mitigation Conference*, Las Vegas, Nevada, October 7-11, 169-176 (1985).
6. R.R. YOUNGS, F.H. SWAN, M.S. POWER, D.P. SCHWARTZ, and R.K. GREEN, "Probabilistic Analysis of Earthquake Ground Shaking Hazard Along the Wasatch Front, Utah: Assessment of Regional Earthquake Hazards and Risk



Along the Wasatch Front, Utah," *U.S. Geological Survey Open File Report 87-585, II*, M-1-110 (1987).

7. K.J. COPPERSMITH, and R.R. YOUNGS, "Capturing Uncertainty in Probabilistic Seismic Hazard Assessments Within Intraplate Environments," *Proceedings of the 3rd National Conference on Earthquake Engineering, Charleston, South Carolina, August 24-28, I*, 301-312 (1986).

8. D.I. DOSER and R.B. SMITH, "An Assessment of source parameters of earthquakes in the Cordillera of the Western United States," *Bulletin of the Seismological Society of America*, 79, 1383-1409 (1989).

9. D.P. SCHWARTZ, K.J. COPPERSMITH, and F.H. SWAN, III, "Methods for estimating maximum earthquake magnitudes," *Proceedings of the Eight World Conference on Earthquake Engineering, I*, 279-285 (1984).

10. D. WELLS, and K.J. COPPERSMITH, "New Earthquake Magnitude and Fault Rupture Parameters: Part I Surface Rupture Length and Rupture Area Relationships," *Seismological Research Letters*, 60, 27, paper submitted to Journal of Geophysical Research.

11. J.G. Anderson, "Estimating the Seismicity from Geological Structure for Seismic Risk Studies," *Bulletin of the Seismological Society of America*, 69, 135-158 (1979).

12. R.R. YOUNGS, and K.J. COPPERSMITH, "Implications of Fault Slip Rates and Earthquake Recurrence Models to Probabilistic Seismic Hazard Estimates," *Bulletin of the Seismological Society of America*, 75, 939-964 (1985).

13. D. GIBSON, L.E. SHEPHARD, F.H. SWAN, J.R. WESLING, and F.A. KERL, "Synthesis of Studies for the Potential of Fault Rupture at the Proposed Surface Facilities, Yucca Mountain, Nevada," *Proceedings of the International Topical Meeting on High Level Radioactive Waste Management, I*, 109-116 (1990).